Am J Transl Res 2024;16(8):4083-4100
www.ajtr.org /ISSN:1943-8141/AJTR0152226

Original Article

NCKAP1 as a prognostic and immunological biomarker: pan-cancer analysis and validation in renal clear cell carcinoma

Xiao Liang[1*], Aonan Hong[1*], Ruizhi Shen[2], Minmin Zhu[3], Weiqian Tian[1]

[1]Affiliated Hospital of Nanjing University of Chinese Medicine, Jiangsu Province Hospital of Chinese Medicine, Nanjing 210000, Jiangsu, China; [2]Department of Oncology, Jiangnan University Medical Center, Wuxi 214002, Jiangsu, China; [3]Department of Anesthesiology, Jiangnan University Medical Center, Wuxi 214002, Jiangsu, China. [*]Equal contributors.

Received July 14, 2023; Accepted August 14, 2024; Epub August 15, 2024; Published August 30, 2024

Abstract: Objectives: To systematically investigate the expression, prognostic value, genetic alterations, immune infiltration, and molecular function of Nck-associated protein 1 (NCKAP1) in a pan-cancer analysis, with a specific focus on its association with kidney renal cell carcinoma (KIRC). Methods: We analyzed the role of NCKAP1 across various tumor types using data from The Cancer Genome Atlas (TCGA). The Gene Expression Profiling Interactive Analysis version 2 (GEPIA2) database was used to assess the correlation between NCKAP1 expression levels and overall survival (OS) and disease-free survival (DFS) across different cancers, as well as its association with cancer stage. Genetic alterations of NCKAP1 were explored using CBioPortal, and their prognostic implications were assessed. NCKAP1 was further analyzed through Gene Ontology and protein interaction network analyses. Immunohistochemistry (IHC) staining from the Human Protein Atlas (HPA) database evaluated NCKAP1 levels in KIRC tissues. Functional assays, including Cell Counting Kit-8 (CCK-8), colony formation, transwell, and wound healing assays, were conducted to determine the effects of NCKAP1 overexpression on cell growth rate and their ability to invade, proliferate, migrate in a KIRC (786-O) cell line. The relationship between NCKAP1 expression and immune infiltration in KIRC was systematically examined using the Tumor Immune Estimation Resource. Results: NCKAP1 expression was significantly altered in most tumor types compared to corresponding non-tumor tissues. Survival analysis indicated that low NCKAP1 expression was associated with poor OS, DFS, and advanced cancer stage ($P < 0.05$) specifically in KIRC. Genetic alterations in NCKAP1 were linked to clinical outcome in cancer patients, and a positive correlation was observed between NCKAP1 expression and cancer-associated fibroblast infiltration ($P < 0.05$). Gene Ontology analysis revealed that NCKAP1 regulates the actin cytoskeleton and interacts with proteins such as CYFIP1, ABI2, WASF2, and BRK1. IHC staining showed significantly lower NCKAP1 levels in KIRC tissues compared to normal tissues. Overexpression of NCKAP1 in KIRC cell lines reduced cell proliferation, invasion, and migration ($P < 0.05$). NCKAP1 was also positively correlated with macrophage, neutrophil, and CD4+ T cell infiltration ($P < 0.001$). Conclusion: NCKAP1 may serve as a prognostic and immunological marker and may be a therapeutic target for KIRC.

Keywords: Nck-associated protein 1, prognosis, pan-cancer, biomarker, kidney, renal clear cell carcinoma

Introduction

Cancer affects hundreds of millions of people worldwide, with clinical outcome depending on multiple factors, including the availability of reliable biomarkers [1, 2]. As personalized medicine advances, biomarkers derived from DNA, RNA, and proteins are becoming increasingly important [3]. Identifying oncogenes is crucial for understanding carcinogenesis and tumor progression, thereby broadening treatment options [4]. The development of the Cancer Genome Atlas (TCGA) in the last decade has significantly expanded our ability to analyze pan-cancer data [5, 6].

Nck-associated protein 1 (NCKAP1) is a component of the WASF regulatory complex (WRC), which includes CYFIP1, ABI2, WASF2, and BRK1. It may function as a transducing protein

https://doi.org/10.62347/UKQB2042

in the Rac signaling pathway, a positive regulator of Arp2/3 complex-mediated actin nucleation, and a mediator of a novel form of cell death called disulfideptosis [7, 8]. According to Kwon et al., inhibiting NCKAP1 expression reduced cell migration and invasion in colorectal cancer, suggesting its role in epithelial-mesenchymal transition (EMT) and its potential as a biomarker for detecting metastatic colorectal cancer and developing therapeutic strategies [9]. Additionally, NCKAP1 plays a critical role in HSP90-induced invasion and metastasis by activating MMP9 and promoting EMT in non-small-cell lung cancer cells [10]. In a mouse melanoma model, NCKAP1 depletion led to increased collagen deposition, fibrotic stroma, reduced tumor proliferation, and enhanced immune infiltration, ultimately slowing tumor growth [11]. Furthermore, in hepatocellular carcinoma (HCC) cell lines, NCKAP1 promotes cell invasion by binding to WASF1 and modulates the cell cycle through Rb1/p53 regulation, contributing to HCC carcinogenesis [12]. Therefore, NCKAP1 may serve as an important biomarker for cancer prognosis and treatment. To our knowledge, no comprehensive analysis of NCKAP1's function and clinical significance at the pan-cancer level has been conducted.

In this study, we systematically investigated the expression, prognostic value, genetic alterations, immune infiltration, and molecular function of NCKAP1 across various cancers, with a specific focus on its association with kidney renal cell carcinoma (KIRC).

Materials and methods

Gene expression analysis

NCKAP1 mRNA expression was analyzed using the Human Protein Atlas (HPA) database (version 20.1) (https://www.proteinatlas.org/). Gene expression analysis in tumor and non-tumor tissues was performed using the "Gene DE" module in Tumor Immune Estimation Resource version 2 (TIMER2, http://timer.cistrome.org/). This analysis aimed to determine whether there are differences in NCKAP1 expression between normal and tumor tissues.

Survival prognosis analysis

The survival prognosis of NCKAP1 was assessed using Kaplan-Meier plots for overall survival (OS) and disease-free survival (DFS). A survival significance map of NCKAP1 across all TCGA tumor types was generated using the "Survival Analysis" module in Gene Expression Profiling Interactive Analysis version 2 (GEPIA2, http://gepia2.cancer-pku.cn/), using the Log-rank test (Mantel-Cox test) for hypothesis testing. The Cox proportional hazard ratio and 95% confidence interval were included in survival plots.

Genetic alteration analysis

Genetic alterations in NCKAP1 were analyzed using the cBio Cancer Genomics Portal (CBioPortal, https://www.cbioportal.org/). This tool provided information on the frequency of gene mutations and copy number alterations across various cancer types, calculated using the "Cancer Types Summary" module based on TCGA pan-cancer datasets. A mutation site plot was generated with the "Mutations" module. The relationship between NCKAP1 mutation status and prognosis in cervical squamous cell carcinoma (CSCC) and lung adenocarcinoma (LUAD) was examined by categorizing cases based on molecular profiles and generating a survival plot based on the presence of copy number alterations (altered and unaltered groups).

Immune cell infiltration analysis

The Tumor Immune Estimation Resource (TIMER) online platform, using RNA-Seq expression profiling data, was employed to analyze immune cell infiltration in different tumor tissues and its impact on clinical outcome. We used the TIMER2.0 "Immune" module to investigate the correlation between NCKAP1 expression and cancer-associated fibroblast infiltration using the Extended Polydimensional Immunome Characterization (EPIC) and Tumor Immune Dysfunction and Exclusion (TIDE) algorithms. Additionally, we assessed the relationship between NCKAP1 expression and immune cell infiltration, including B cells, CD8+ T cells, CD4+ T cells, macrophages, neutrophils, and dendritic cells in KIRC, using partial Spearman's correlation for this association analysis.

Gene enrichment analysis

We used the STRING tool (https://string-db.org/) to construct a co-expression network for Homo sapiens NCKAP1 and analyzed 100 gene

symbols correlated with NCKAP1, extracted via the "Similar Gene Detection" module in GEPIA2. Gene Ontology pathway enrichment analysis was performed using the "clusterProfiler" R package (version 4.6.0). Additionally, pairwise gene correlation analysis was conducted using the "Correlation Analysis" module in GEPIA2, employing Pearson, Spearman, and Kendall methods to assess gene expression correlations.

Protein interaction and conservation analysis

We created an NCKAP1-protein interaction network using the BioGRID Network module (https://thebiogrid.org/), with the layout set to "Concentric Circles". Gene communication between vertebrates was visualized using the UCSC Genome Browser (http://genome.ucsc.edu/cgi-bin/hgTracks).

Pathologic sample collection

Paraffin-embedded KIRC tissue samples and matched normal tissues were collected and examined by immunohistochemistry (IHC) with NCKAP1 antibody from the HPA database to compare NCKAP1 expression differences between normal tissue and renal clear cell carcinoma.

Cell culture and transfections

The KIRC 786-0 cell line used in this study was obtained from The American Type Culture Collection (ATCC, United States). Cells were cultured in RPMI-1640 medium (Gibco, USA) with 10% fetal bovine serum (FBS; Gibco, United States) and maintained in an incubator with 5% CO_2 at 37°C. The NCKAP1 overexpression vector and control vector were provided by Hanbio Biotechnology Co., Ltd. (Shanghai, China). Transfections into 786-0 cells were performed using Lipofectamine 2000 and Opti-MEMI medium (Gibco, United States), following the manufacturer's instructions for successful gene delivery and expression.

qRT-PCR analysis

Total RNA was extracted using Trizol reagent (Thermo Fisher, United States), and cDNA was synthesized using the RevertAid First Strand cDNA Synthesis Kit (Thermo Scientific, United States). Quantitative real-time PCR (qRT-PCR) was conducted in triplicate using SYBR Green I (Servicebio, China) to assess NCKAP1 expression levels. GAPDH served as the internal control. The primers used for qRT-PCR were as follows: NCKAP1: 5'-TCCTAAATACTGACGCTACAGCA-3' (forward) and 5'-GCCTCCTTGCATTCTCTTATGTC-3' (reverse); GAPDH: 5'-GTCTCCTCTGACTTCAACAGCG-3' (forward) and 5'-ACCACCCTGTTGCTGTAGCCAA-3' (reverse).

Western blot analysis

Proteins were extracted using a whole-cell lysis assay (Servicebio, China). After separation through sodium dodecyl sulfate-polyacrylamide gel electrophoresis (SDS-PAGE), proteins were transferred to polyvinylidene difluoride (PVDF) membranes for western blotting. Membranes were blocked with skimmed milk and then incubated overnight at 4°C with a primary antibody against NCKAP1 (1:1,000; CST, United States). The following day, membranes were incubated with a secondary antibody (1:5,000; Abcam, UK) at room temperature after washing. Protein bands were detected using a chemiluminescence detection kit. GAPDH (1:1,000; CST, United States) was used as the loading control to ensure equal protein loading across samples.

Cell viability assay

Cell viability was assessed using the Cell Counting Kit-8 (Beyotime, China) following the manufacturer's protocol. Cells were seeded into 96-well plates at a density of 2×10^3 cells per well and cultured for 72 hours under standard conditions. At 24, 48, and 72 hours, 10 µL of CCK-8 solution was added to each well, followed by incubation at 37°C for 2 hours. Absorbance was measured at 540 nm to determine cell viability. Each experiment was performed in triplicate and repeated three times to ensure accuracy.

Colony formation assay

Cells were plated at a density of 5×10^2 per well in 6-well plates and incubated at 37°C. After two weeks of culture, colonies were fixed with 4% paraformaldehyde and stained with 0.5% crystal violet at room temperature. Colony counting was performed by analyzing digital images of the wells from each of the three replicate plates.

Transwell assay

Cell invasion was assessed using Transwell inserts (8 μm pore size, Corning, United States) coated with Matrigel (BD, United States). A total of 5×10^4 cells were placed in the upper chamber, with RPMI-1640 medium supplemented with 20% FBS added to the lower chamber. After 24 hours of incubation, cells that had migrated to the lower chamber were fixed and stained. The number of invading cells was counted in five randomly chosen fields of view on the lower membrane. The experiment was conducted in triplicate to ensure reliability.

Wound healing assay

To assess cell migration capability, 5×10^5 cells were seeded into 24-well plates and allowed to adhere overnight. Once the cells reached confluence, artificial wounds were created by scratching a line down the center of the cell layer. The cells were then maintained in serum-free medium. Wounded areas were photographed immediately (0 hour) and at 36 hours post-wounding using an Olympus inverted microscope. The experiment was performed in triplicate.

Statistical analysis

All experiments were conducted in triplicate, and the data were analyzed using Prism GraphPad 8.0 software. Results were presented as mean ± standard deviation (SD). Differences between groups were assessed using the t-test, with statistical significance set as $P < 0.05$.

Results

Gene expression analysis of NCKAP1

Analysis of datasets from the HPA, Genotype-Tissue Expression (GTEx) and function annotation of the mammalian genome (FANTOM5) revealed that NCKAP1 was highly expressed in muscle tissues, such as heart and skeletal muscle, and was enriched in parathyroid gland (**Figure 1A-C**). Single-cell RNA-seq data also indicated high NCKAP1 expression in excitatory and inhibitory neurons (**Figure 1D**). Further, NCKAP1 mRNA expression was found to be altered in various tumor tissues compared to corresponding normal tissues. Significantly lower NCKAP1 expression was observed in breast invasive carcinoma (BRCA), kidney Chromophobe (KICH), KIRC, kidney renal papillary cell carcinoma (KIRP), prostate adenocarcinoma (PRAD), skin Cutaneous Melanoma (SKCM) (all $P < 0.001$), uterine corpus endometrial (UCEC) ($P < 0.01$), bladder Urothelial Carcinoma (BLCA) and glioblastoma multiforme (GBM) ($P < 0.05$) when compared to normal tissue (**Figure 1E**). Besides, when compared to these normal tissues, NCKAP1 expression was also significantly elevated in cholangiocarcinoma (CHOL), liver hepatocellular carcinoma (LIHC), LUAD, lung squamous cell carcinoma (all $P < 0.001$), head and neck squamous cell carcinoma (HNSC) ($P < 0.01$), esophageal carcinoma (ESCA) and stomach adenocarcinoma (STAD) (both $P < 0.05$) (**Figure 1E**).

Association between NCKAP1 expression and cancer prognosis

To evaluate the prognostic value of NCKAP1, we used GEPIA2 to correlate NCKAP1 expression with patient prognosis across various tumors based on TCGA datasets. Lower NCKAP1 expression was associated with shorter OS in KIRC ($P = 2 \times 10^{-4}$), while higher NCKAP1 expression was linked to shorter OS in LIHC ($P = 3.7 \times 10^{-2}$) and cervical squamous cell carcinoma (CESC) ($P = 2 \times 10^{-2}$) (**Figure 2A-D**). Additionally, DFS analysis revealed that low NCKAP1 expression was an indicator of poor outcome in patients with adrenocortical carcinoma (ACC) ($P = 5 \times 10^{-3}$) and uveal melanoma (UVM) ($P = 3.2 \times 10^{-2}$). Conversely, higher NCKAP1 expression was associated with better outcome in KIRC ($P = 3.8 \times 10^{-2}$) and brain low-grade glioma (LGG) ($P = 1.8 \times 10^{-2}$) (**Figure 2E-I**).

Correlation between NCKAP1 expression and pathologic stages of tumors

The relationship between NCKAP1 expression and pathologic stages of tumors was analyzed using GEPIA2. NCKAP1 expression was found to vary across tumor stages in KIRC ($P = 0.00174$), LIHC ($P = 0.0484$), LUAD ($P = 0.0459$), COAD ($P = 0.0462$) and OV ($P = 0.00205$). In particular, low expression of NCKAP1 was significantly correlated with advanced stages of KIRC ($P = 0.00174$) and OV ($P = 0.00205$) (**Figure 3A-E**).

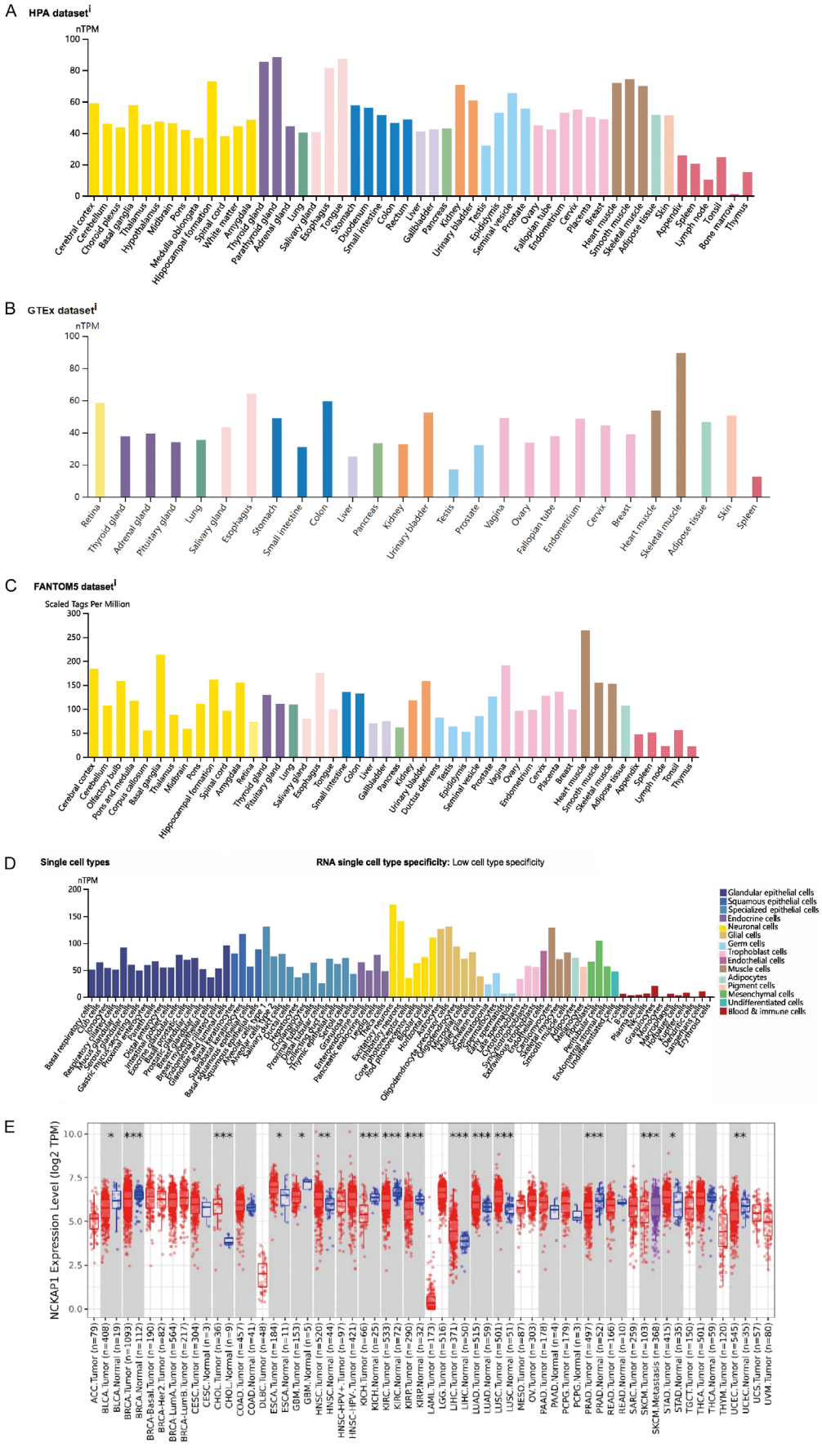
A
HPA dataset
nTPM
B
GTEx dataset
nTPM
C
FANTOM5 dataset
Scaled Tags Per Million
D
Single cell types
RNA single cell type specificity: Low cell type specificity
nTPM
Glandular epithelial cells
Squamous epithelial cells
Specialized epithelial cells
Endocrine cells
Neuronal cells
Glial cells
Germ cells
Trophoblast cells
Endothelial cells
Muscle cells
Adipocytes
Pigment cells
Mesenchymal cells
Undifferentiated cells
Blood & immune cells
E
NCKAP1 Expression Level (log2 TPM)

Figure 1. NCKAP1 expression status in different normal tissues, cell types, and tumors. A-C. NCKAP1 expression based on datasets of the HPA, GTEx and FANTOM5 in different normal tissues. D. NCKAP1 expression in various cell types. E. NCKAP1 expression status in different tumors and normal tissues visualized by TIMER2.0. *P < 0.05; **P < 0.01; ***P < 0.001. NCKAP1, Nck-associated protein 1; HPA, Human protein atlas; GTEx, Genotype-Tissue Expression; FANTOM5, Function annotation of the mammalian genome 5; TIMER2.0, Tumor Immune Estimation Resource version 2.

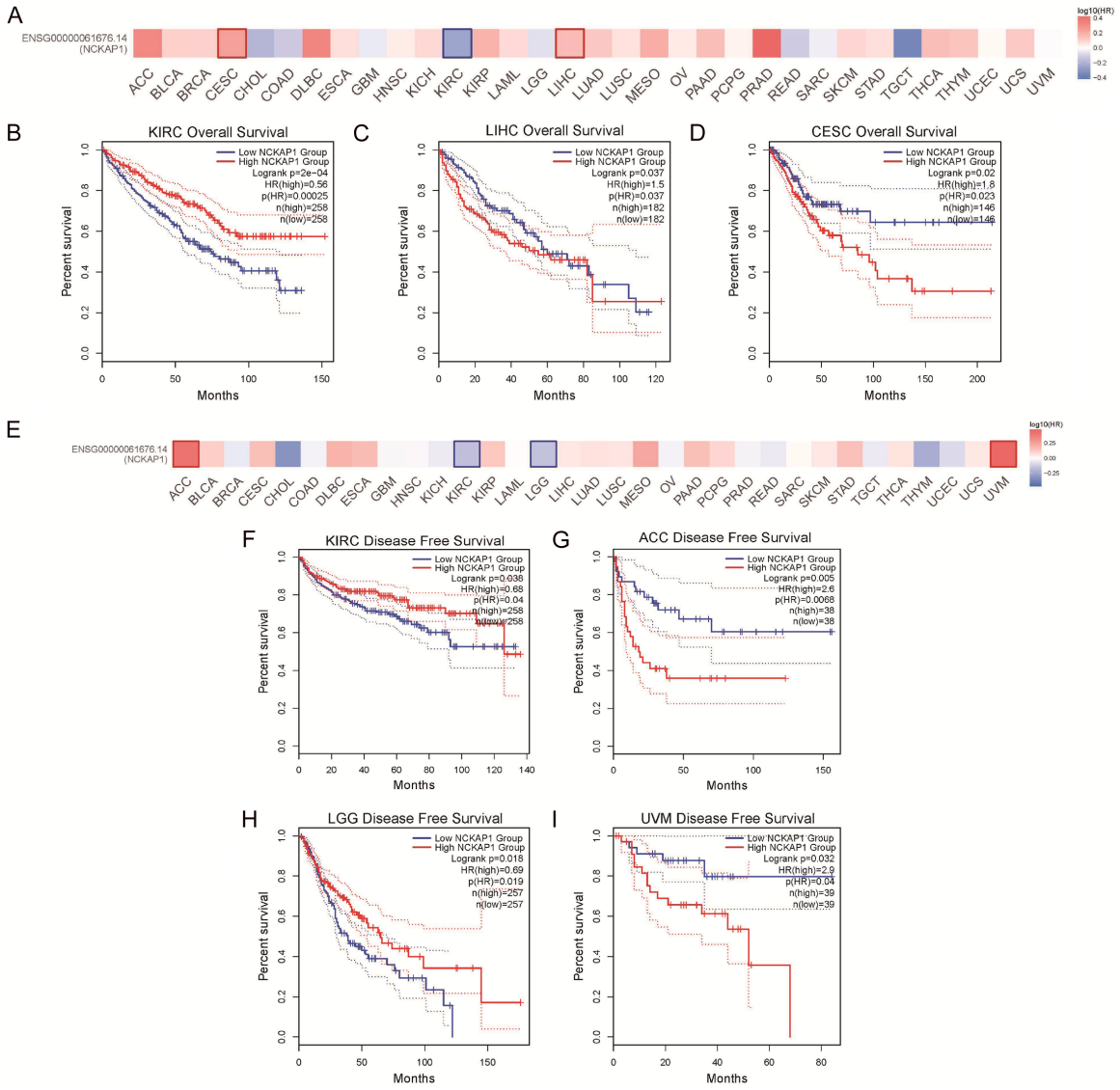

Figure 2. Correlation between NCKAP1 expression and overall survival in patients with different TCGA tumor types. GEPIA2 was used to build a survival map (A) and conduct overall survival analyses (B-D). Correlation between NCKAP1 expression and disease-free survival in patients with different TCGA tumor types. GEPIA2 was used to build a survival map (E) and conduct disease-free survival (F-I) analyses. The survival map and Kaplan-Meier plots with significant results are displayed. The 95% confidence intervals of OS and DFS are indicated by red and blue dotted lines for high and low NCKAP1 groups, respectively. NCKAP1, Nck-associated protein 1; TCGA, The Cancer Genome Atlas; GEPIA2, Gene Expression Profiling Interactive Analysis version 2; OS, overall survival; DFS, disease-free survival.

Tumor-specific genetic alterations of NCKAP1

Genetic alterations in NCKAP1 were investigated across various tumor types using cBioPortal, based on TCGA datasets. A higher frequency of genetic modifications was observed in uterine carcinosarcoma (UCS) tumor samples, with mutations and amplifications being the pri-

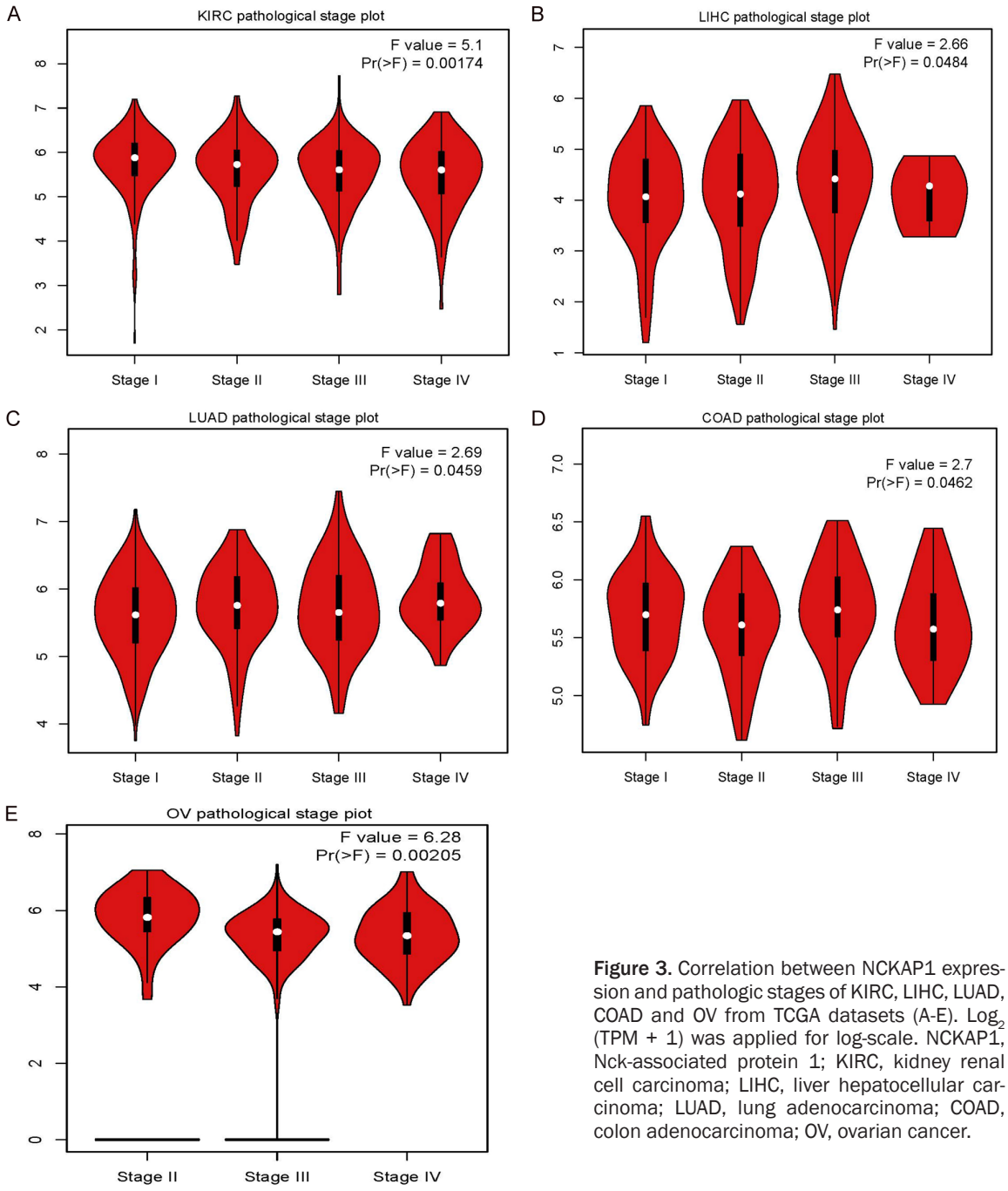

Figure 3. Correlation between NCKAP1 expression and pathologic stages of KIRC, LIHC, LUAD, COAD and OV from TCGA datasets (A-E). Log_2 (TPM + 1) was applied for log-scale. NCKAP1, Nck-associated protein 1; KIRC, kidney renal cell carcinoma; LIHC, liver hepatocellular carcinoma; LUAD, lung adenocarcinoma; COAD, colon adenocarcinoma; OV, ovarian cancer.

mary genetic abnormalities (**Figure 4A**). In total, 176 mutations of NCKAP1 were identified across TCGA tumor samples, including 141 missense mutations, 20 truncating mutations, 5 fusion mutations, 9 splicing mutations, and 1 inframe mutation (**Figure 4B**). Additionally, NCKAP1 amplification was associated with prognosis in CSCC patients in terms of PFS ($P = 2.29 \times 10^{-2}$) and LUAD patients in terms of PFS ($P = 2.84 \times 10^{-2}$) (**Figure 4C**, **4D**).

Correlation analysis between NCKAP1 and cancer-associated fibroblast infiltration

Cancer-associated fibroblasts, a key component of the dense stromal tumor microenvironment, contribute to the extracellular matrix [13]. To explore the correlation between cancer-associated fibroblast infiltration and NCKAP1 expression in different cancer types, we utilized the EPIC and TIDE algorithms. A posi-

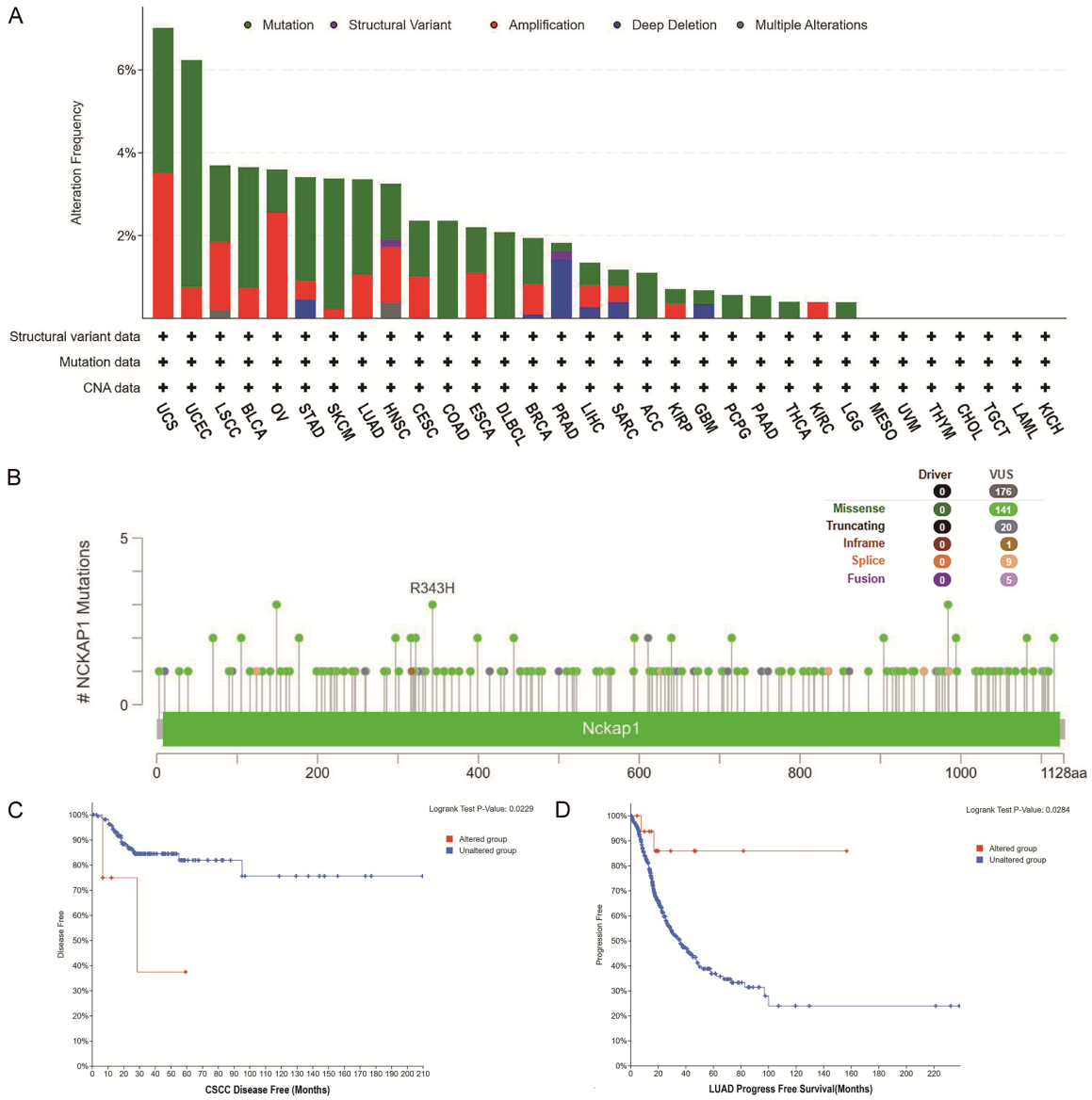

Figure 4. NCKAP1 genetic alteration in various tumor types in the TCGA. The alteration frequency with NCKAP1 genetic alteration type (A) and NCKAP1 mutation site (B) were generated by cBioPortal. The correlations between NCKAP1 amplification status and disease-free survival of CSCC (C) were analyzed by cBioPortal. The correlation between mutation status and overall survival, and progression-free survival of LUAD (D) was analyzed by cBioPortal. NCKAP1, Nck-associated protein 1; TCGA, The Cancer Genome Atlas; KIRC, kidney renal cell carcinoma; LIHC, liver hepatocellular carcinoma; LUAD, lung adenocarcinoma; COAD, colon adenocarcinoma; OV, ovarian cancer; UCS, uterine carcinosarcoma; BRCA, breast invasive carcinoma; KICH, kidney chromophobe; KIRP, kidney renal papillary cell carcinoma; PRAD, prostate adenocarcinoma; SKCM, skin cutaneous melanoma; UCEC, uterine corpus endometrial; BLCA, bladder urothelial carcinoma; GBM, glioblastoma multiforme; LGG, lower grade glioma; LSCC, laryngeal squamous cell carcinoma; STAD, stomach adenocarcinoma; HNSC, head and neck squamous cell carcinoma; ESCA, esophageal carcinoma; DLBCL, diffuse large B-cell lymphoma; SARC, sarcoma; PCPG, pheochromocytoma and paraganglioma; CHOL, cholangiocarcinoma; PAAD, pancreatic adenocarcinoma; THCA, thyroid carcinoma; MESO, mesothelioma; THYM, thymoma; LAML, acute myeloid leukemia.

tive correlation was observed between NCKAP1 expression and cancer-associated fibroblast infiltration in ACC, BRCA, cervical squamous cell carcinoma and endocervical adenocarcinoma (CESC), LGG, and STAD (all $P < 0.001$) (**Figure 5**).

NCKAP1-related gene enrichment analysis

To investigate the functional mechanism of NCKAP1 in carcinogenesis, we used GEPIA2 to extract the top 100 genes with expression patterns similar to NCKAP1 from the TCGA datas-

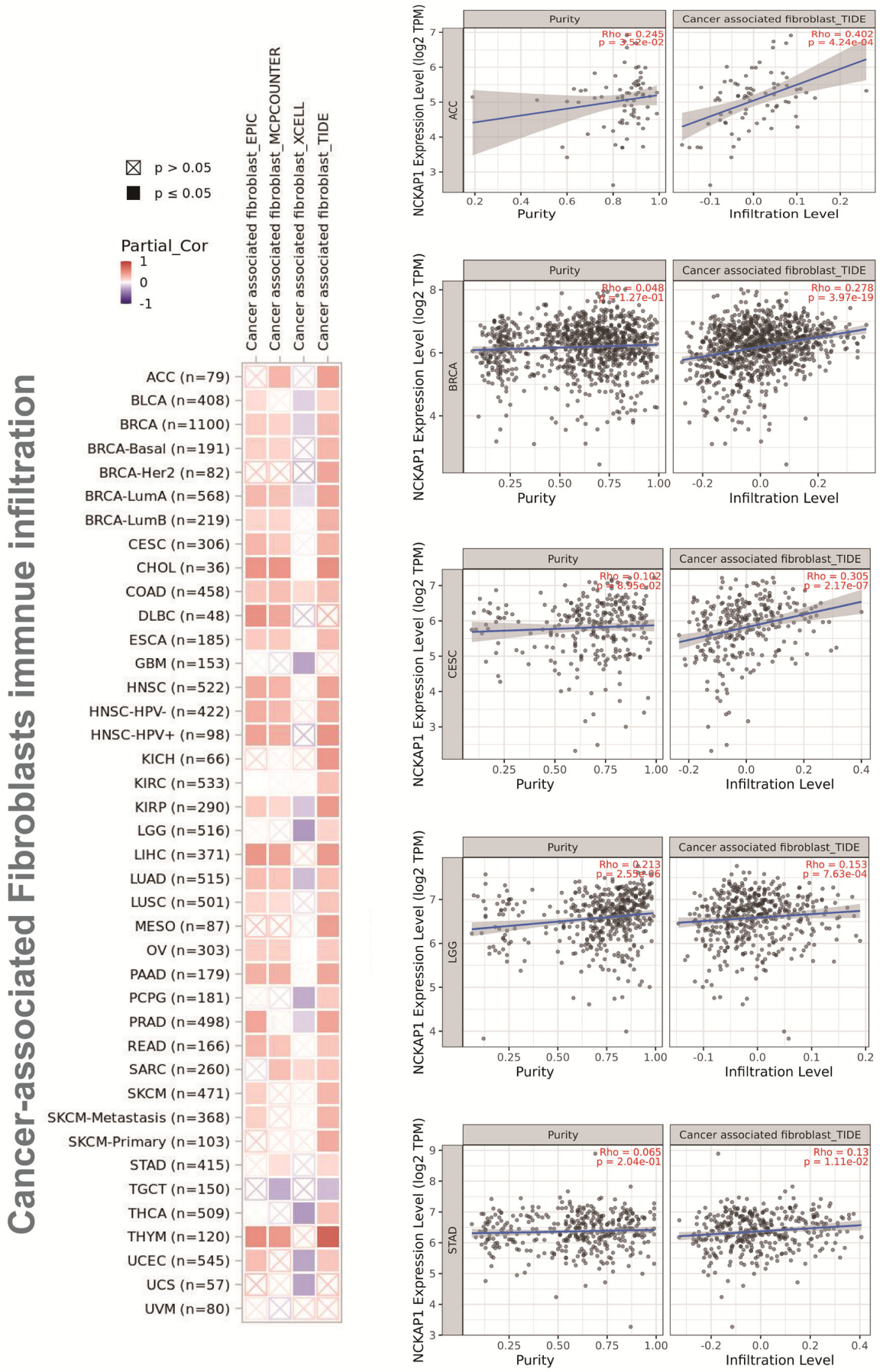
Cancer-associated Fibroblasts immnue infiltration
Cancer associated fibroblast_EPIC
Cancer associated fibroblast_MCPCOUNTER
Cancer associated fibroblast_XCELL
Cancer associated fibroblast_TIDE
p > 0.05
p ≤ 0.05
Partial_Cor
1
0
-1
ACC (n=79)
BLCA (n=408)
BRCA (n=1100)
BRCA-Basal (n=191)
BRCA-Her2 (n=82)
BRCA-LumA (n=568)
BRCA-LumB (n=219)
CESC (n=306)
CHOL (n=36)
COAD (n=458)
DLBC (n=48)
ESCA (n=185)
GBM (n=153)
HNSC (n=522)
HNSC-HPV- (n=422)
HNSC-HPV+ (n=98)
KICH (n=66)
KIRC (n=533)
KIRP (n=290)
LGG (n=516)
LIHC (n=371)
LUAD (n=515)
LUSC (n=501)
MESO (n=87)
OV (n=303)
PAAD (n=179)
PCPG (n=181)
PRAD (n=498)
READ (n=166)
SARC (n=260)
SKCM (n=471)
SKCM-Metastasis (n=368)
SKCM-Primary (n=103)
STAD (n=415)
TGCT (n=150)
THCA (n=509)
THYM (n=120)
UCEC (n=545)
UCS (n=57)
UVM (n=80)
Purity
Cancer associated fibroblast_TIDE
ACC
Rho = 0.245
p = 3.52e-02
Rho = 0.402
p = 4.24e-04
BRCA
Rho = 0.048
p = 1.27e-01
Rho = 0.278
p = 3.97e-19
CESC
Rho = 0.102
p = 8.95e-02
Rho = 0.305
p = 2.17e-07
LGG
Rho = 0.213
p = 2.55e-06
Rho = 0.153
p = 7.63e-04
STAD
Rho = 0.065
p = 2.04e-01
Rho = 0.13
p = 1.11e-02
NCKAP1 Expression Level (log2 TPM)
Purity
Infiltration Level

Figure 5. Correlation between NCKAP1 expression and cancer-associated fibroblast immune infiltration. EPIC and TIDE algorithms were used to calculate the correlation between NCKAP1 expression and cancer-associated fibroblast immune infiltration in all tumor types from TCGA. NCKAP1, Nck-associated protein 1; EPIC, Extended Polydimensional Immunome Characterization; TIDE, Tumor Immune Dysfunction and Exclusion; TCGA, The Cancer Genome Atlas.

ets (Supplementary Table 1). Gene Ontology enrichment analysis discovered that these genes were related to the regulation of the actin cytoskeleton (**Figure 6A**). Additionally, 50 genes co-expressed with NCKAP1 were identified using the STRING tool, further confirming their enrichment in actin cytoskeleton regulation (Supplementary Table 2 and **Figure 6B**). These findings suggest that NCKAP1 may contribute to these biologic processes through its interactions with actin cytoskeleton regulatory proteins. The BioGRID 4.4.219 database showed physical interactions between NCKAP1 and CYFIP1, WASF2, BRK1, and ABI2 (**Figure 6C**), and the expression levels of NCKAP1 were significantly correlated with those of CYFIP1, ABI2, and WASF2 (**Figure 6D-G**). Furthermore, the expression of CYFIP1, WASF2, ABI2, and C3ORF10 (BRK1) mRNAs also changed in various tumor tissues compared to corresponding normal tissues (**Figure 7A-D**). Taking these results into account, we speculate that NCKAP1 may play a tumor-inhibiting role in cancers by regulating actin cytoskeleton function facilitating cell disulfidptosis.

Reduced expression of NCKAP1 in KIRC

We performed IHC staining of four cases of KIRC tissues paired with normal tissues from the HPA database to identify the expression of NCKAP1. The cohort included one female (age: 56 years), one male (age: 59 years) with KIRC, and one female (age: 70 years), one male (age: 56 years) with normal kidney. IHC results indicated that NCKAP1 was expressed in the cytoplasm/membranous structures of normal tubules; however, NCKAP1 expression was not detected in the tumor cells of KIRC tissues (**Figure 8**).

Overexpression of NCKAP1 suppressed cell growth in 786-0 cells

The reduced expression of NCKAP1 was significantly correlated with various clinicopathologic characteristics, indicating that NCKAP1 may play a crucial role in KIRC tumor development. To validate this, 786-0 cells were transfected with either an NCKAP1 overexpression plasmid (pEZ-Lv201-NCKAP1) or a control vector (pEZLv201). Post-transfection, qRT-PCR and western blot analysis confirmed the elevated levels of NCKAP1 mRNA and protein, respectively (**Figure 9A**, **9B**). As illustrated in **Figure 9C**, the overexpression of NCKAP1 in 786-0 cells resulted in a significant reduction in cell growth rate ($P < 0.01$).

Overexpression of NCKAP1 inhibits proliferation, migration, and invasion of 786-0 cells

To assess the role of NCKAP1, we examined the proliferation, migration, and invasion capabilities of 786-0 cells overexpressing NCKAP1. **Figure 10A** showed that NCKAP1-overexpressing cells formed fewer and smaller colonies compared to the vector control group ($P < 0.01$). Moreover, overexpression of NCKAP1 led to reduced wound closure ($P < 0.01$) (**Figure 10B**) and decreased invasiveness ($P < 0.01$) (**Figure 10C**) in comparison to vector controls. These results indicated that NCKAP1 significantly affects the proliferation, migration, and invasion of 786-0 cells.

Correlation analysis between NCKAP1 and immune cells infiltration in KIRC

We utilized the TCGA database via TIMER2.0 to investigate the clinical correlation between the NCKAP1 expression and tumor immune cells infiltration in KIRC. Our results indicated a positive correlation between NCKAP1 expression and infiltration of macrophages ($P = 3.13 \times 10^{-16}$), neutrophils ($P = 3.78 \times 10^{-8}$), CD4+ T cells ($P = 6.53 \times 10^{-6}$). However, there was no association with B cells ($P = 8.90 \times 10^{-2}$), CD8+ T cells ($P = 4.77 \times 10^{-1}$), or Myeloid dendritic cell ($P = 4.38 \times 10^{-1}$) infiltration in KIRC (**Figure 11**).

Discussion

The dual-luciferase reporter assay has identified that Circ_NCKAP1 promotes the progression of skin basal cell carcinoma (BCC) by sponging the miR-148b-5p/HSP90 axis [14].

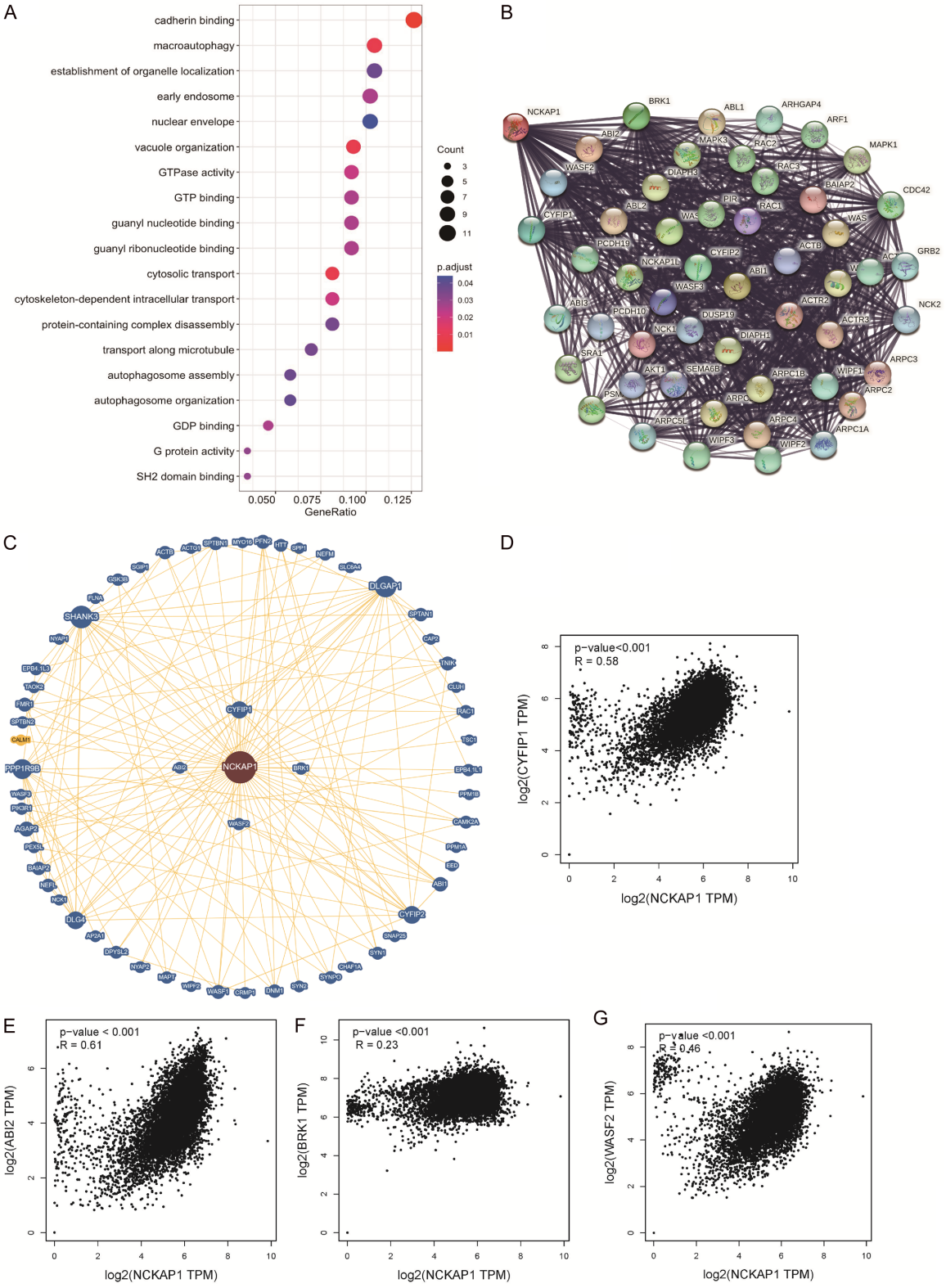

Figure 6. NCKAP1-related gene enrichment analysis. A. Gene Ontology (GO) analysis of the top 100 genes co-expressed with NCKAP1 obtained by the GEPIA2. B. Co-expression network of 50 genes co-expressed with NCKAP1 obtained by the STRING tool. C. NCKAP1-protein interactions obtained by BioGRID. D-G. Correlation analysis between NCKAP1 and CYFIP1, WASF2, ABI2 and BRK1 conducted by GEPIA2 across all tumor samples from TCGA. NCKAP1, Nck-associated protein 1; TCGA, The Cancer Genome Atlas; GEPIA2, Gene Expression Profiling Interactive Analysis version 2.

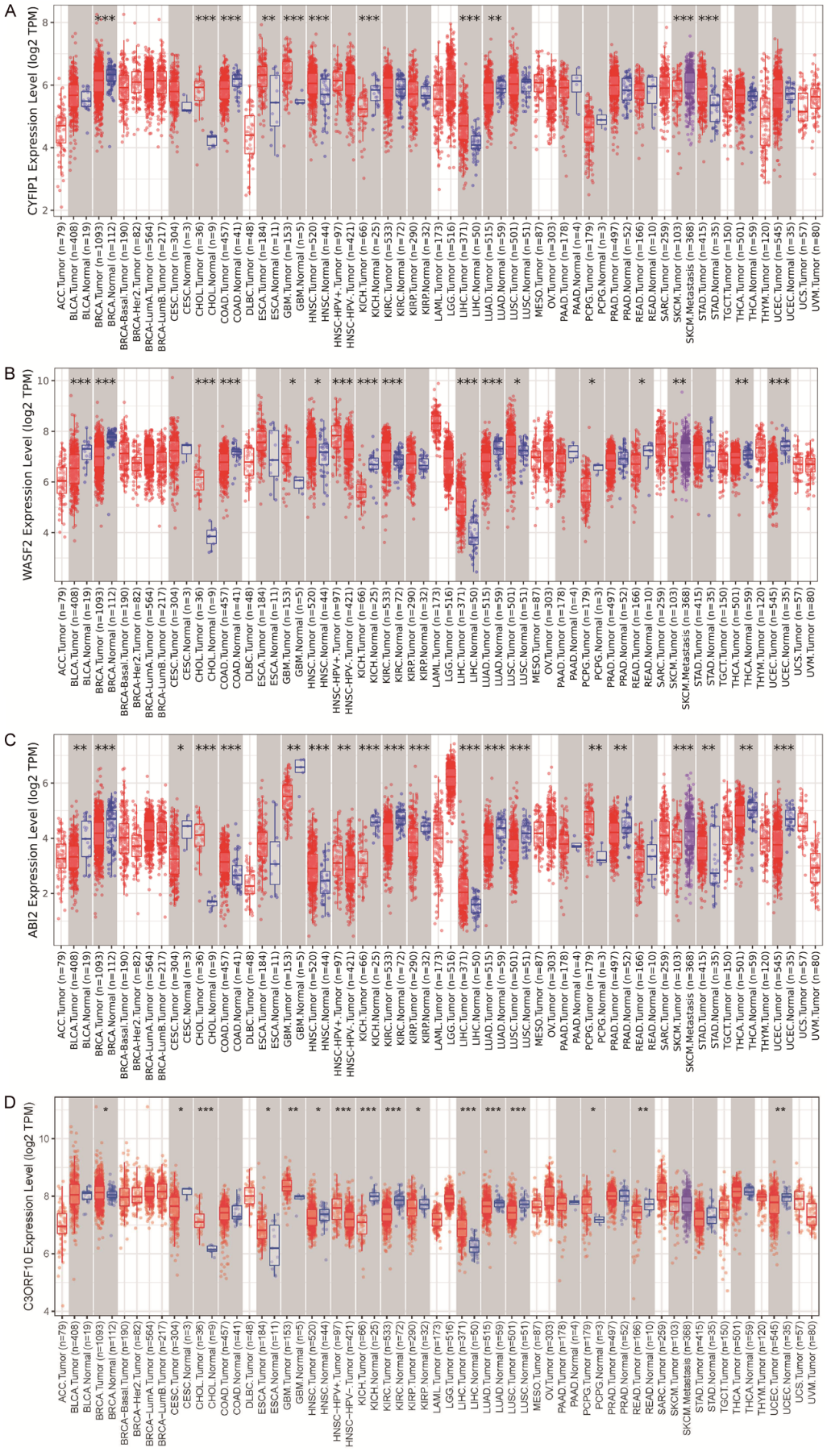
A
CYFIP1 Expression Level (log2 TPM)
B
WASF2 Expression Level (log2 TPM)
C
ABI2 Expression Level (log2 TPM)
D
C3ORF10 Expression Level (log2 TPM)
ACC.Tumor (n=79)
BLCA.Tumor (n=408)
BLCA.Normal (n=19)
BRCA.Tumor (n=1093)
BRCA.Normal (n=112)
BRCA-Basal.Tumor (n=190)
BRCA-Her2.Tumor (n=82)
BRCA-LumA.Tumor (n=564)
BRCA-LumB.Tumor (n=217)
CESC.Tumor (n=304)
CESC.Normal (n=3)
CHOL.Tumor (n=36)
CHOL.Normal (n=9)
COAD.Tumor (n=457)
COAD.Normal (n=41)
DLBC.Tumor (n=48)
ESCA.Tumor (n=184)
ESCA.Normal (n=11)
GBM.Tumor (n=153)
GBM.Normal (n=5)
HNSC.Tumor (n=520)
HNSC.Normal (n=44)
HNSC-HPV+.Tumor (n=97)
HNSC-HPV-.Tumor (n=421)
KICH.Tumor (n=66)
KICH.Normal (n=25)
KIRC.Tumor (n=533)
KIRC.Normal (n=72)
KIRP.Tumor (n=290)
KIRP.Normal (n=32)
LAML.Tumor (n=173)
LGG.Tumor (n=516)
LIHC.Tumor (n=371)
LIHC.Normal (n=50)
LUAD.Tumor (n=515)
LUAD.Normal (n=59)
LUSC.Tumor (n=501)
LUSC.Normal (n=51)
MESO.Tumor (n=87)
OV.Tumor (n=303)
PAAD.Tumor (n=178)
PAAD.Normal (n=4)
PCPG.Tumor (n=179)
PCPG.Normal (n=3)
PRAD.Tumor (n=497)
PRAD.Normal (n=52)
READ.Tumor (n=166)
READ.Normal (n=10)
SARC.Tumor (n=259)
SKCM.Tumor (n=103)
SKCM.Metastasis (n=368)
STAD.Tumor (n=415)
STAD.Normal (n=35)
TGCT.Tumor (n=150)
THCA.Tumor (n=501)
THCA.Normal (n=59)
THYM.Tumor (n=120)
UCEC.Tumor (n=545)
UCEC.Normal (n=35)
UCS.Tumor (n=57)
UVM.Tumor (n=80)

Figure 7. CYFIP1, WASF2, ABI2, and C3ORF10 (BRK1) expression status in different normal tissues. A-D. The expression status of CYFIP1, WASF2, ABI2, and BRK1 in different tumor types was visualized by TIMER2.0. *P < 0.05; **P < 0.01; ***P < 0.001. ACC, adrenocortical carcinoma; LGG, lower grade glioma; BLCA, bladder urothelial carcinoma; KIRC, kidney renal cell carcinoma; LIHC, liver hepatocellular carcinoma; LUAD, lung adenocarcinoma; COAD, colon adenocarcinoma; OV, ovarian cancer; UCS, uterine carcinosarcoma; BRCA, breast invasive carcinoma; KICH, kidney chromophobe; KIRP, kidney renal papillary cell carcinoma; PRAD, prostate adenocarcinoma; SKCM, skin cutaneous melanoma; UCEC, uterine corpus endometrial; GBM, glioblastoma multiforme; LGG, lower grade glioma; LSCC, laryngeal squamous cell carcinoma; STAD, stomach adenocarcinoma; HNSC, head and neck squamous cell carcinoma; ESCA, esophageal carcinoma; DLBCL, diffuse large B-cell lymphoma; SARC, sarcoma; PCPG, pheochromocytoma and paraganglioma; CHOL, cholangiocarcinoma; PAAD, pancreatic adenocarcinoma; THCA, thyroid carcinoma; MESO, mesothelioma; THYM, thymoma; LAML, acute myeloid leukemia.

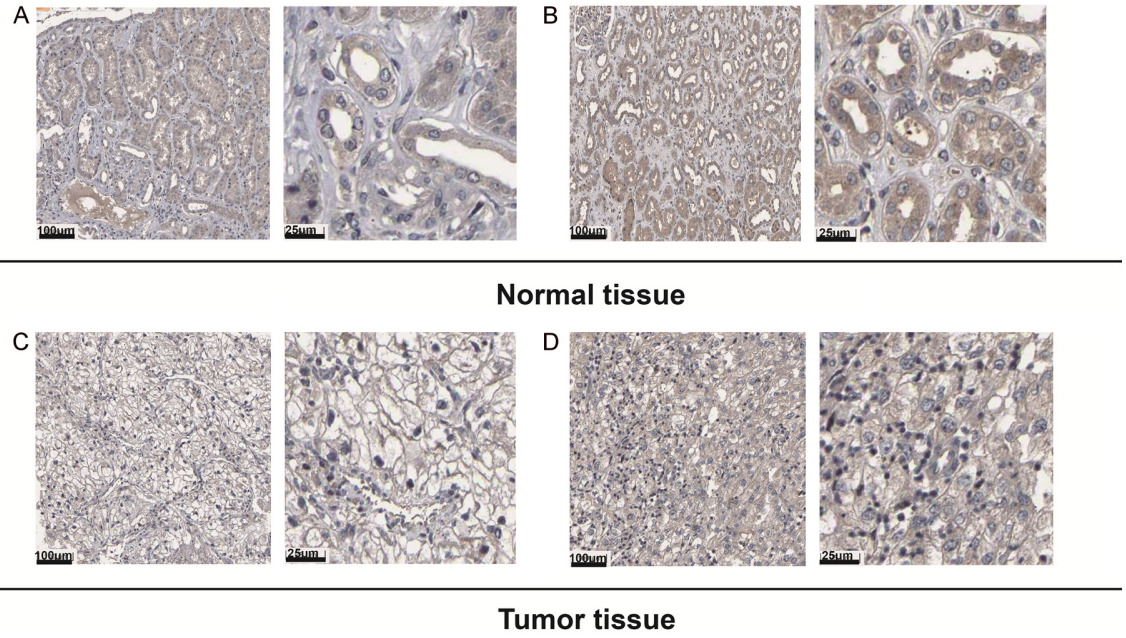

Figure 8. Representative images of NCKAP1 expression in KIRC tissues and normal tissues. IHC staining for KIRC tissues of one female (age: 56 years) (A), one male (age: 59 years) (B), and normal tissues of one female (age: 70 years) (C), one male (age: 56 years) (D) from HPA database. Scale bar = 100 μm or 25 μm. NCKAP1, Nck-associated protein 1; KIRC, kidney renal cell carcinoma; HPA, Human Protein Atlas.

Similarly, Qing Ma's study found that overexpression of miR-140-5p in patients with aortic dissection inhibits NCKAP1 expression, leading to reduced proliferation, migration, and invasion of vascular smooth muscle cells [15]. In hepatocellular carcinoma (HCC), high NCKAP1 expression is significantly associated with low miR-34c-3p expression and correlates with a favorable prognosis [16]. Additionally, NCKAP1 has been identified as one of the five independent risk factors in a disulfidptosis-related genes (DRGs) model for prognostic evaluation of lung adenocarcinoma (LUAD). The high area under the receiver operating characteristic curve (AUC) and C-index of this model indicate its stable and reliable predictive effect on LUAD prognosis [17]. Despite these findings, the significance of NCKAP1 across various tumor types had not been comprehensively explored.

In this study, we systematically characterized NCKAP1 across 33 TCGA tumor types by analyzing features such as immune infiltration, genetic alterations, and gene expression. Our pan-cancer analysis suggests that NCKAP1 may serve as a prospective prognostic marker and a therapeutic target for KIRC.

NCKAP1 mutations were most prevalent in uterine corpus endometrial carcinoma (UCEC), followed by skin cutaneous melanoma (SKCM), bladder urothelial carcinoma (BLCA), stomach adenocarcinoma (STAD), and colon adenocarcinoma (COAD). Our analysis revealed that NCKAP1 alterations may act as a risk factor for

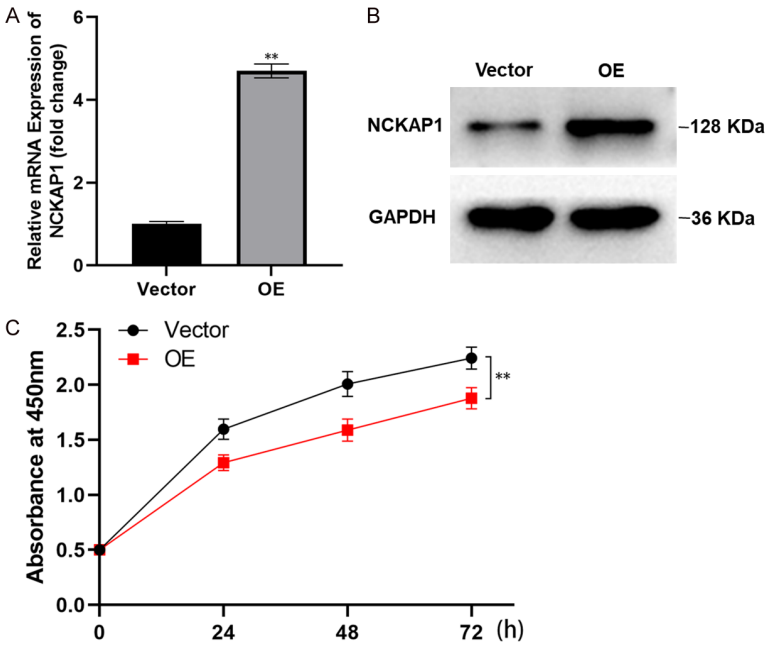

Figure 9. NCKAP1 overexpression in 786-O cell line suppressed the cell growth rate. Overexpression of NCKAP1 (OE) in a transfected 786-O cell line verified by qPCR (A) and western blot (B) compared to that of 786-O cells transfected with the control vector (Vector). GAPDH was used as a loading control. (C) CCK-8 assay results showed the cell viability in 786-O-OE cells compared to 786-O-Vector cells. NCKAP1, Nck-associated protein 1; CCK-8, Cell Counting Kit-8.

cervical squamous cell carcinoma (CSCC) patients, while potentially serving as a protective factor for LUAD patients. The TCGA program has provided extensive cancer genomics data, offering unprecedented opportunities to identify molecular aberrations in pan-cancer studies [18]. Our findings show that NCKAP1 is expressed in various tissues but is downregulated in BRCA, BLCA, GBM, PRAD, KIRC, KIRP, KICH, UCEC, and SKCM. Notably, low NCKAP1 expression is associated with poor DFS and OS specifically in KIRC, and is significantly linked to advanced cancer stages, suggesting a role in malignant progression. IHC staining revealed that NCKAP1 levels were significantly lower in KIRC tissues compared to normal tissues from the HPA database. These results are consistent with Chen's findings, which showed that NCKAP1 is significantly downregulated in KIRC and correlated with advanced clinicopathologic features and poor prognosis [19]. Furthermore, our in vitro experiments demonstrated that overexpression of NCKAP1 in KIRC cell lines reduced cell growth, invasion, proliferation, and migration.

Genomic profiling has identified numerous genomic variants as significant cancer biomarkers, which could be developed into large-scale clinical studies [20]. Therefore, NCKAP1 may become a promising biomarker for the management or prognosis of KIRC. Additionally, the interaction between immune cells and cancer cells is crucial for cancer migration and metastasis [21, 22]. We demonstrated that NCKAP1 is positively correlated with various types of immune cell infiltration, including macrophages, neutrophils, and CD4+ T cells in KIRC. Existing literature also highlights the role of NCKAP1 in the immune microenvironment [23].

In addition, we utilized STRING and GEPIA2 to identify genes co-expressed with NCKAP1 across various tumors and tissues. Gene enrichment analysis indicated a strong association with the regulation of actin cytoskeleton function, consistent with previous studies [24-28]. NCKAP1 physically interacts with key actin cytoskeleton genes, including CYFIP1, WASF2, ABI2, and BRK1. The expression of CYFIP1, ABI2, and WASF2 is highly correlated with NCKAP1 expression, further supporting our gene enrichment analysis. Activation of the WASF protein complex occurs through interaction with RAC1, and the Rac1-WASF3 complex no longer binds when NCKAP1 is inactivated [29]. NCKAP1 deficiency leads to partial resistance to disulfidptosis, likely involving disulfide bonding in multiple proteins, possibly including actin cytoskeleton proteins [8]. Activation of the WRC, including NCKAP1, promotes actin cross-linking, which is essential for the formation of lamellipodia and invadopodia, structures frequently used in cancer metastasis and invasion [30]. High expression of the NCKAP1 subunit of the Arp2/3-activating WAVE complex is associated with poor metastasis-free survival (MFS) in breast cancer, in contrast to the expression of Arpin, the Arp2/3 inhibitory

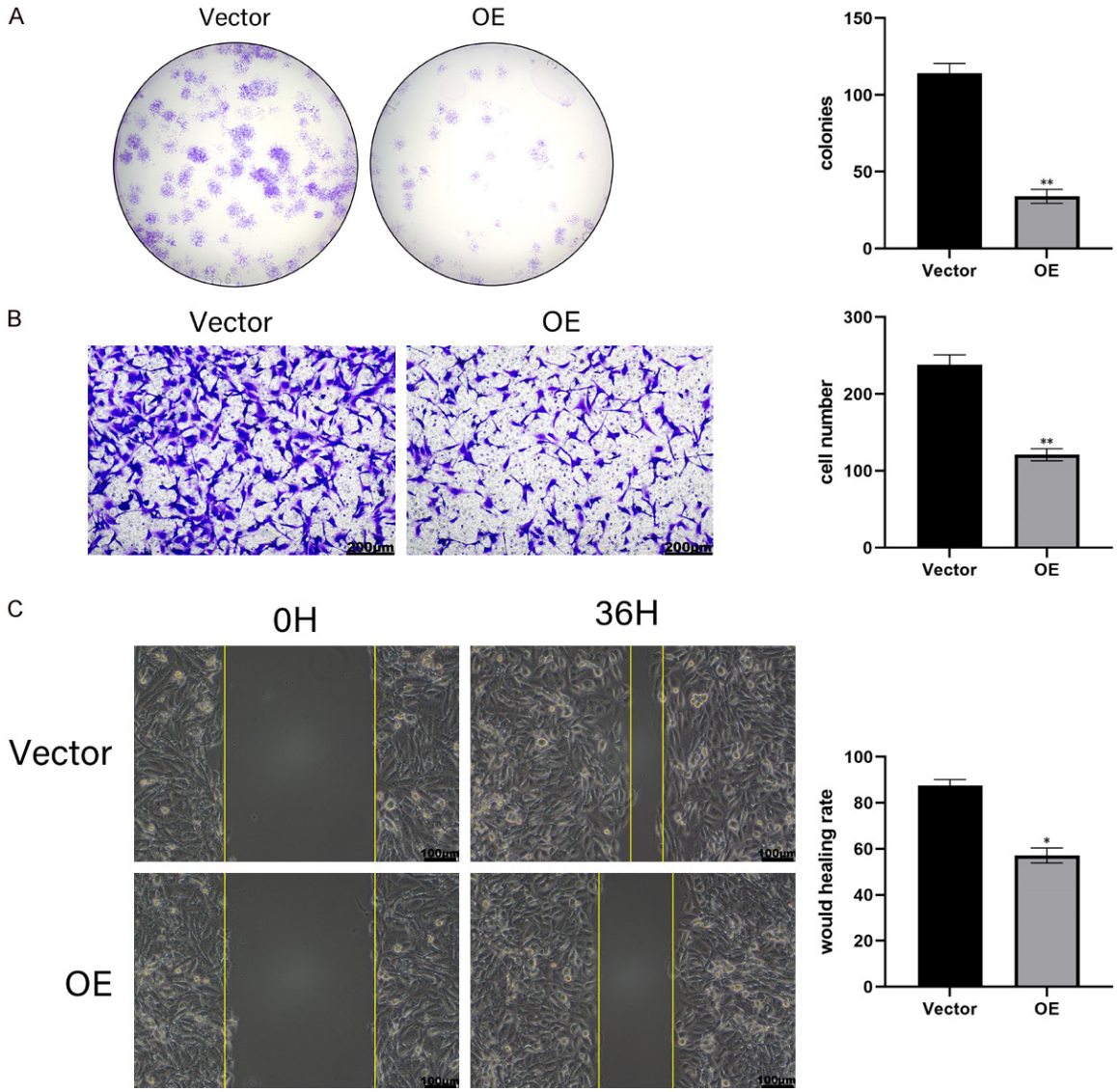

Figure 10. NCKAP1 inhibited proliferation, migration, and invasion in vitro. Cell colony formation assay showed a statistically significant decrease of (A) 786-0-OE cells compared to 786-0-Vector cells. Wound-healing assay results showed a significant decrease of migration (B) 786-0-OE cells compared to 786-0-Vector cells. Scale bar = 200 μm. Transwell invasion assay results showed a significant decrease of invaded (C) 786-0-OE cells compared to 786-0-Vector cells. Scale bar = 100 μm. The results are mean ± SD values from three independent experiments. *P < 0.05; **P < 0.01. NCKAP1, Nck-associated protein 1.

protein [31]. Targeting the peptide at the interface between CYFIP1 and NCKAP1 has been shown to inhibit the metastasis and progression of lung and liver cancer cells [32]. Based on these findings, we hypothesize that glucose and disulfide may coordinately regulate actin cytoskeleton disulfide formation, leading to lamellipodia formation through the WRC, including NCKAP1 and other subunits in KIRC cells (**Figure 12**).

This study has limitations, including the small sample sizes for rare tumor types, which may lead to inaccurate results. The findings linking NCKAP1 to cancer progression are preliminary and require further experimental validation to determine its precise molecular role in tumorigenesis. Additionally, only bioinformatic analyses were conducted, and no relevant basic experiments were performed. Validation experiments were limited to a single tumor cell line,

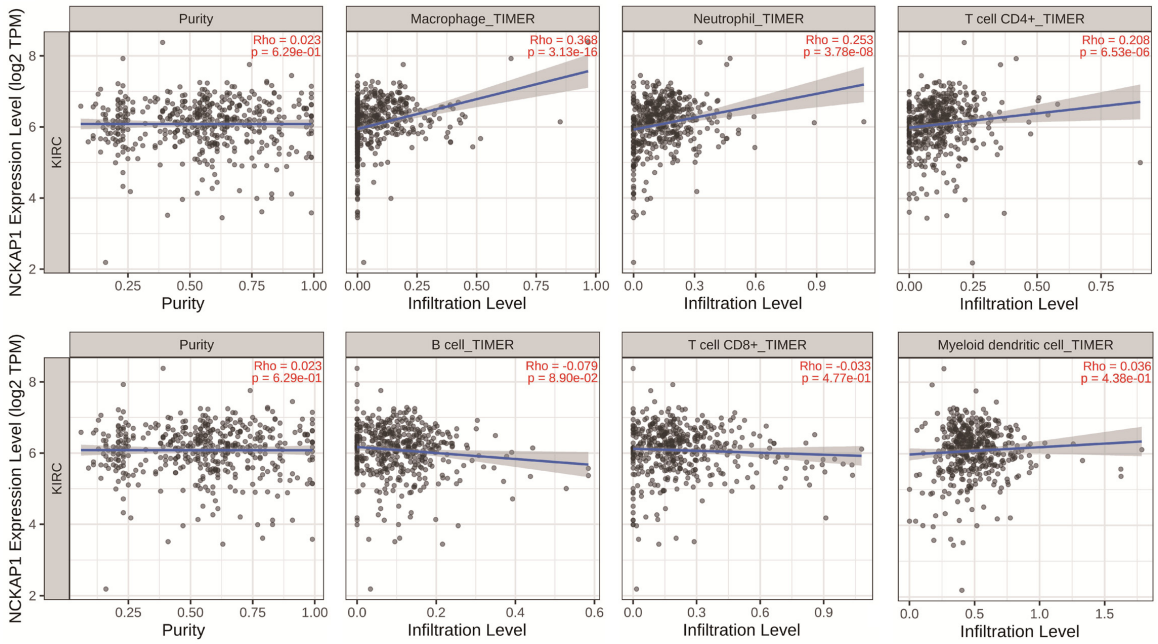

Figure 11. Correlation analysis between NCKAP1 expression and immune cell infiltration in KIRC. The clinical association between macrophages, neutrophils, CD4+ T cells, B cells, CD8+ T cells, myeloid dendritic cell infiltration, and NCKAP1 expression in KIRC was investigated using TIMER2.0 from TCGA database. NCKAP1, Nck-associated protein 1; KIRC, kidney renal cell carcinoma; TIMER2.0, Tumor Immune Estimation Resource version 2; TCGA, The Cancer Genome Atlas.

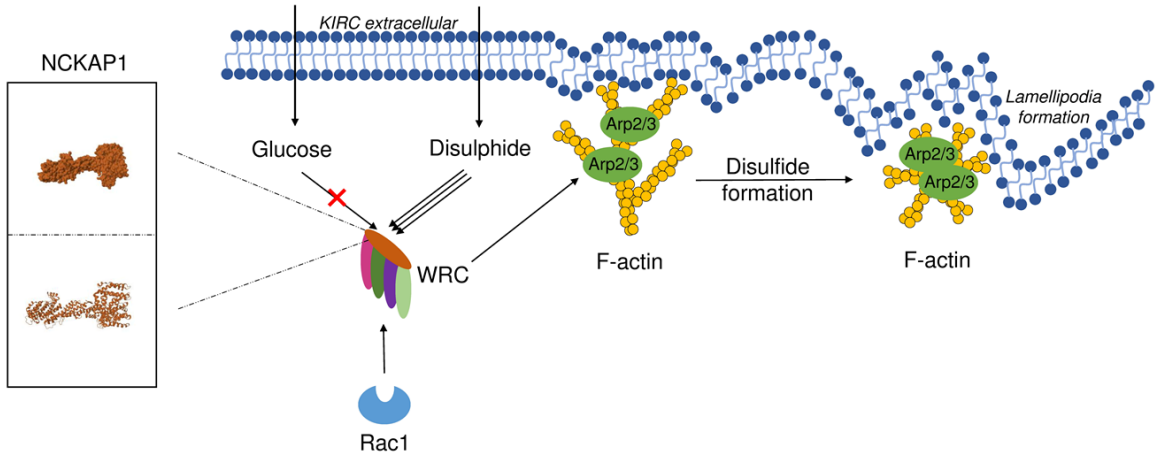

Figure 12. Working model depicting how glucose and disulphide coordinately regulate the disulfide formation of the actin cytoskeleton formatting lamellipodia by WRC including NCKAP1 and other subunits in KIRC cells. NCKAP1, Nck-associated protein 1; KIRC, kidney renal cell carcinoma; WRC, WAVE Regulatory Complex.

and should be extended to more diverse cell lines. Concurrent in vivo experiments are also necessary.

In conclusion, while NCKAP1 expression is low in many cancers, it is specifically associated with poor DFS and OS only in KIRC, and correlates with advanced cancer stages, suggesting a role in malignant progression in KIRC. Overexpression of NCKAP1 in KIRC cell lines decreased cell growth, invasion, proliferation, and migration. Therefore, NCKAP1 may be a biomarker for the management and prognosis of KIRC. Additionally, NCKAP1 showed a notable positive correlation with immune cell infiltration, including macrophages, neutrophils,

and CD4+ T cells in KIRC, suggesting that it may play a role in regulating disulfidptosis and tumor immunity. Further research is needed to explore the functionality of NCKAP1, particularly in KIRC.

Acknowledgements

This study was supported by the funds from Guiding Project of Qinghai Provincial Health Commission (2023-wjzdx-99), Science Popularization Work Creation Project of Wuxi Municipal Health Commission (P202310), Research Project of Jiangsu Province Maternal and Child Health Association (FYX202011), and Traditional Chinese Medicine Science and Technology Development Program (YB2020044).

Disclosure of conflict of interest

None.

Address correspondence to: Weiqian Tian, Affiliated Hospital of Nanjing University of Chinese Medicine, Jiangsu Province Hospital of Chinese Medicine, Nanjing 210000, Jiangsu, China. Tel: +86-13914764426; E-mail: twq1972@163.com; Minmin Zhu, Department of Anesthesiology, Jiangnan University Medical Center, Wuxi 214002, Jiangsu, China. Tel: +86-13921292032; E-mail: mmzhummzhu@163.com

References

[1] Davalos V and Esteller M. Cancer epigenetics in clinical practice. CA Cancer J Clin 2023; 73: 376-424.

[2] Galeano Nino JL, Wu H, LaCourse KD, Kempchinsky AG, Baryiames A, Barber B, Futran N, Houlton J, Sather C, Sicinska E, Taylor A, Minot SS, Johnston CD and Bullman S. Effect of the intratumoral microbiota on spatial and cellular heterogeneity in cancer. Nature 2022; 611: 810-817.

[3] Kim B, Kang SY and Kim KM. DNA-protein biomarkers for immunotherapy in the era of precision oncology. J Pathol Transl Med 2021; 55: 26-32.

[4] Kim WR, Park EG, Lee DH, Lee YJ, Bae WH and Kim HS. The tumorigenic role of circular RNA-microRNA axis in cancer. Int J Mol Sci 2023; 24: 3050.

[5] Chen X, Zhang D, Jiang F, Shen Y, Li X, Hu X, Wei P and Shen X. Prognostic prediction using a stemness index-related signature in a cohort of gastric cancer. Front Mol Biosci 2020; 7: 570702.

[6] Cheng X, Wang X, Nie K, Cheng L, Zhang Z, Hu Y and Peng W. Systematic pan-cancer analysis identifies TREM2 as an immunological and prognostic biomarker. Front Immunol 2021; 12: 646523.

[7] Limaye AJ, Whittaker MK, Bendzunas GN, Cowell JK and Kennedy EJ. Targeting the WASF3 complex to suppress metastasis. Pharmacol Res 2022; 182: 106302.

[8] Liu X, Nie L, Zhang Y, Yan Y, Wang C, Colic M, Olszewski K, Horbath A, Chen X, Lei G, Mao C, Wu S, Zhuang L, Poyurovsky MV, James You M, Hart T, Billadeau DD, Chen J and Gan B. Actin cytoskeleton vulnerability to disulfide stress mediates disulfidptosis. Nat Cell Biol 2023; 25: 404-414.

[9] Kwon MR, Lee JH, Park J, Park SS, Ju EJ, Ko EJ, Shin SH, Son GW, Lee HW, Kim YJ, Song SY, Jeong SY and Choi EK. NCK-associated protein 1 regulates metastasis and is a novel prognostic marker for colorectal cancer. Cell Death Discov 2023; 9: 7.

[10] Xiong Y, He L, Shay C, Lang L, Loveless J, Yu J, Chemmalakuzhy R, Jiang H, Liu M and Teng Y. Nck-associated protein 1 associates with HSP90 to drive metastasis in human non-small-cell lung cancer. J Exp Clin Cancer Res 2019; 38: 122.

[11] Swaminathan K, Campbell A, Papalazarou V, Jaber-Hijazi F, Nixon C, McGhee E, Strathdee D, Sansom OJ and Machesky LM. The RAC1 target NCKAP1 plays a crucial role in the progression of Braf;Pten-driven melanoma in mice. J Invest Dermatol 2021; 141: 628-637, e15.

[12] Zhong XP, Kan A, Ling YH, Lu LH, Mei J, Wei W, Li SH and Guo RP. NCKAP1 improves patient outcome and inhibits cell growth by enhancing Rb1/p53 activation in hepatocellular carcinoma. Cell Death Dis 2019; 10: 369.

[13] Sunami Y, Boker V and Kleeff J. Targeting and reprograming cancer-associated fibroblasts and the tumor microenvironment in pancreatic cancer. Cancers (Basel) 2021; 13: 697.

[14] Fan ZX, Xi W, Miao XY, Li LY and Miao GY. Circ_NCKAP1 promotes skin basal cell carcinoma progression by sponging the miR-148b-5p/HSP90 axis. Eur Rev Med Pharmacol Sci 2021; 25: 5355-5364.

[15] Ma Q, Liu J, Li C and Wang D. miR-140-5p inhibits the proliferation, migration and invasion of vascular smooth muscle cells by suppressing the expression of NCKAP1. Folia Histochem Cytobiol 2021; 59: 22-29.

[16] Xiao CZ, Wei W, Guo ZX, Zhang MY, Zhang YF, Wang JH, Shi M, Wang HY and Guo RP. MicroRNA-34c-3p promotes cell proliferation and invasion in hepatocellular carcinoma by regulation of NCKAP1 expression. J Cancer Res Clin Oncol 2017; 143: 263-273.

[17] Ni L, Yang H, Wu X, Zhou K and Wang S. The expression and prognostic value of disulfidptosis progress in lung adenocarcinoma. Aging (Albany NY) 2023; 15: 7741-7759.
[18] Deng M, Bragelmann J, Schultze JL and Perner S. Web-TCGA: an online platform for integrated analysis of molecular cancer data sets. BMC Bioinformatics 2016; 17: 72.
[19] Chen J, Ge J, Zhang W, Xie X, Zhong X and Tang S. NCKAP1 is a prognostic biomarker for inhibition of cell growth in clear cell renal cell carcinoma. Front Genet 2022; 13: 764957.
[20] Barbar J, Armach M, Hodroj MH, Assi S, El Nakib C, Chamseddine N and Assi HI. Emerging genetic biomarkers in lung adenocarcinoma. SAGE Open Med 2022; 10: 20503121221132352.
[21] Wang C, Deng Z, Zang L, Shu Y, He S and Wu X. Immune cells regulate matrix metalloproteinases to reshape the tumor microenvironment to affect the invasion, migration, and metastasis of pancreatic cancer. Am J Transl Res 2022; 14: 8437-8456.
[22] Nakamura Y, Kinoshita J, Yamaguchi T, Aoki T, Saito H, Hamabe-Horiike T, Harada S, Nomura S, Inaki N and Fushida S. Crosstalk between cancer-associated fibroblasts and immune cells in peritoneal metastasis: inhibition in the migration of M2 macrophages and mast cells by Tranilast. Gastric Cancer 2022; 25: 515-526.
[23] Yan J, Fang Z, Shi M, Tu C, Zhang S, Jiang C, Li Q and Shao Y. Clinical significance of disulfidptosis-related genes and functional analysis in gastric cancer. J Cancer 2024; 15: 1053-1066.
[24] De Rubeis S, Pasciuto E, Li KW, Fernandez E, Di Marino D, Buzzi A, Ostroff LE, Klann E, Zwartkruis FJ, Komiyama NH, Grant SG, Poujol C, Choquet D, Achsel T, Posthuma D, Smit AB and Bagni C. CYFIP1 coordinates mRNA translation and cytoskeleton remodeling to ensure proper dendritic spine formation. Neuron 2013; 79: 1169-1182.
[25] Dubielecka PM, Ladwein KI, Xiong X, Migeotte I, Chorzalska A, Anderson KV, Sawicki JA, Rottner K, Stradal TE and Kotula L. Essential role for Abi1 in embryonic survival and WAVE2 complex integrity. Proc Natl Acad Sci U S A 2011; 108: 7022-7027.
[26] Nowak SJ, Nahirney PC, Hadjantonakis AK and Baylies MK. Nap1-mediated actin remodeling is essential for mammalian myoblast fusion. J Cell Sci 2009; 122: 3282-3293.
[27] Rakeman AS and Anderson KV. Axis specification and morphogenesis in the mouse embryo require Nap1, a regulator of WAVE-mediated actin branching. Development 2006; 133: 3075-3083.
[28] Innocenti M, Zucconi A, Disanza A, Frittoli E, Areces LB, Steffen A, Stradal TE, Di Fiore PP, Carlier MF and Scita G. Abi1 is essential for the formation and activation of a WAVE2 signalling complex. Nat Cell Biol 2004; 6: 319-327.
[29] Teng Y, Qin H, Bahassan A, Bendzunas NG, Kennedy EJ and Cowell JK. The WASF3-NCKAP1-CYFIP1 complex is essential for breast cancer metastasis. Cancer Res 2016; 76: 5133-5142.
[30] Whitelaw JA, Swaminathan K, Kage F and Machesky LM. The WAVE regulatory complex is required to balance protrusion and adhesion in migration. Cells 2020; 9: 1635.
[31] Lomakina ME, Lallemand F, Vacher S, Molinie N, Dang I, Cacheux W, Chipysheva TA, Ermilova VD, de Koning L, Dubois T, Bièche I, Alexandrova AY and Gautreau A. Arpin downregulation in breast cancer is associated with poor prognosis. Br J Cancer 2016; 114: 545-553.
[32] Cowell JK, Teng Y, Bendzunas NG, Ara R, Arbab AS and Kennedy EJ. Suppression of breast cancer metastasis using stapled peptides targeting the WASF regulatory complex. Cancer Growth Metastasis 2017; 10: 1179064417713197.

Supplementary Table 1. Top 100 genes with expression pattern similar to NCKAP1 gene from all tumor types in the TCGA datasets by GEPIA2

Gene Symbol	Gene ID	Pearson Correlation Coefficient
CAMSAP2	ENSG00000118200.14	0.65
SPTLC1	ENSG00000090054.13	0.64
SP3	ENSG00000172845.13	0.63
PRKRA	ENSG00000180228.12	0.63
CWC22	ENSG00000163510.13	0.63
DYNC1I2	ENSG00000077380.15	0.62
ZC3H15	ENSG00000065548.17	0.62
FAM168B	ENSG00000152102.17	0.62
PCNP	ENSG00000081154.11	0.62
EIF4G2	ENSG00000110321.15	0.62
RAB14	ENSG00000119396.10	0.62
ARHGAP5	ENSG00000100852.12	0.61
FUBP3	ENSG00000107164.15	0.61
PUM2	ENSG00000055917.15	0.61
UBQLN1	ENSG00000135018.13	0.61
RAB5A	ENSG00000144566.10	0.61
CRK	ENSG00000167193.7	0.61
RNF11	ENSG00000123091.4	0.61
API5	ENSG00000166181.12	0.6
SMEK2	ENSG00000275052.4	0.6
44992	ENSG00000136536.14	0.6
RPE	ENSG00000197713.14	0.6
CDC42BPB	ENSG00000198752.9	0.6
FBXO3	ENSG00000110429.13	0.6
KPNA4	ENSG00000186432.8	0.6
ARL5A	ENSG00000162980.16	0.6
ZNF770	ENSG00000198146.4	0.59
BTBD1	ENSG00000064726.9	0.59
UBR3	ENSG00000144357.16	0.59
ARHGEF12	ENSG00000196914.8	0.59
NAA30	ENSG00000139977.13	0.59
TNKS2	ENSG00000107854.5	0.59
ZFR	ENSG00000056097.15	0.59
WASL	ENSG00000106299.7	0.59
MATR3	ENSG00000015479.17	0.59
45171	ENSG00000168385.17	0.59
RAB1A	ENSG00000138069.16	0.59
ANKRD13C	ENSG00000118454.12	0.59
BMPR2	ENSG00000204217.12	0.58
PPP2R5E	ENSG00000154001.13	0.58
EXOC5	ENSG00000070367.15	0.58
ABI1	ENSG00000136754.16	0.58
PPP1CB	ENSG00000213639.9	0.58
RAB6A	ENSG00000175582.19	0.58
PURB	ENSG00000146676.6	0.58
GTF2A1	ENSG00000165417.11	0.58
C2orf69	ENSG00000178074.5	0.58
ITGAV	ENSG00000138448.11	0.58
UBQLN2	ENSG00000188021.8	0.58

ARL8B	ENSG00000134108.12	0.58
PTPN11	ENSG00000179295.15	0.58
COPS2	ENSG00000166200.14	0.58
MMGT1	ENSG00000169446.5	0.57
TJP1	ENSG00000104067.16	0.57
HIAT1	ENSG00000156875.13	0.57
FAM199X	ENSG00000123575.8	0.57
HNRNPK	ENSG00000165119.18	0.57
IPO7	ENSG00000205339.9	0.57
GPR107	ENSG00000148358.19	0.57
UEVLD	ENSG00000151116.16	0.57
SMNDC1	ENSG00000119953.12	0.57
ASNSD1	ENSG00000138381.9	0.57
ORC4	ENSG00000115947.13	0.57
NPTN	ENSG00000156642.16	0.57
VPS26A	ENSG00000122958.14	0.57
KPNA1	ENSG00000114030.12	0.57
EIF4H	ENSG00000106682.14	0.57
KCTD18	ENSG00000155729.12	0.57
FYTTD1	ENSG00000122068.12	0.57
FCF1	ENSG00000119616.11	0.56
ICE1	ENSG00000164151.11	0.56
CHMP3	ENSG00000115561.14	0.56
ACBD3	ENSG00000182827.8	0.56
PTK2	ENSG00000169398.19	0.56
SEC24B	ENSG00000138802.11	0.56
GOPC	ENSG00000047932.13	0.56
YWHAQ	ENSG00000134308.13	0.56
UBXN4	ENSG00000144224.16	0.56
KIF5B	ENSG00000170759.10	0.56
CLASP1	ENSG00000074054.17	0.56
ZMYND11	ENSG00000015171.18	0.56
DLG1	ENSG00000075711.20	0.56
FBXW11	ENSG00000072803.17	0.56
MAP4K3	ENSG00000011566.14	0.56
ATP2A2	ENSG00000174437.16	0.56
LINC00657	ENSG00000260032.1	0.56
ZBTB6	ENSG00000186130.4	0.56
TMEM30A	ENSG00000112697.15	0.56
EFCAB14	ENSG00000159658.10	0.56
WDR44	ENSG00000131725.13	0.56
NAB1	ENSG00000138386.16	0.56
FAM175B	ENSG00000165660.7	0.55
MTPN	ENSG00000105887.10	0.55
WDR82	ENSG00000164091.11	0.55
EPC2	ENSG00000135999.11	0.55
45179	ENSG00000186522.14	0.55
KIF1BP	ENSG00000198954.6	0.55
GTF3C4	ENSG00000125484.11	0.55
RAB18	ENSG00000099246.16	0.55
NARS	ENSG00000134440.11	0.55

Supplementary Table 2. GO biological process (BP), cellular component (CC), molecular function (MF) enrichment analysis of 50 co-expressed genes of NCKAP1 derived by STRING tool

ID	ONTOLOGY	Description	Gene Ratio	Bg Ratio	*p* value	p.adjust	q value	Gene ID	Count
GO:0007033	BP	Vacuole organization	8/86	213/18903	5.69E-06	0.008340253	0.007484	51552/29979/5868/5861/29978/55207/51652/488	8
GO:0016482	BP	Cytosolic transport	7/86	171/18903	1.29E-05	0.008340253	0.007484	51552/5868/5870/55207/9559/51652/3799	7
GO:0016236	BP	Macroautophagy	9/86	317/18903	1.39E-05	0.008340253	0.007484	10558/29979/5868/5861/29978/55207/9559/51652/488	9
GO:0030705	BP	Cytoskeleton-dependent intracellular transport	7/86	208/18903	4.55E-05	0.020493416	0.018389457	1781/8976/5861/5870/55207/3799/23291	7
GO:0032984	BP	Protein-containing complex disassembly	7/86	242/18903	0.000117573	0.035384795	0.03175201	23271/29979/51652/3799/23332/488/136319	7
GO:0010970	BP	Transport along microtubule	6/86	168/18903	0.000117753	0.035384795	0.03175201	1781/5861/5870/55207/3799/23291	6
GO:0000045	BP	Autophagosome assembly	5/86	110/18903	0.000145801	0.037313866	0.033483033	29979/5868/5861/29978/488	5
GO:0051656	BP	Establishment of organelle localization	9/86	437/18903	0.000165563	0.037313866	0.033483033	8976/5861/10640/5870/51652/3799/23332/1739/23291	9
GO:1905037	BP	Autophagosome organization	5/86	117/18903	0.000194692	0.039003261	0.034998985	29979/5868/5861/29978/488	5
GO:0005769	CC	Early endosome	9/88	414/19869	9.07E-05	0.025843567	0.021858455	51552/5868/26994/5861/93380/57720/9559/51652/55754	9
GO:0005635	CC	Nuclear envelope	9/88	488/19869	0.000309494	0.044102948	0.037302217	23369/3840/80351/9782/10527/3836/51652/23190/23291	9
GO:0045296	MF	Cadherin binding	11/87	333/18432	4.68E-07	0.000118777	0.000102386	55854/1982/5861/659/10006/5781/7082/3190/7458/3799/1739	11
GO:0003924	MF	GTPase activity	8/87	331/18432	0.000169415	0.021515672	0.018546455	51552/394/5868/26225/5861/5870/55207/22931	8
GO:0019003	MF	GDP binding	4/87	73/18432	0.000393187	0.025872868	0.022302348	51552/5868/55207/22931	4
GO:0005525	MF	GTP binding	8/87	379/18432	0.00042143	0.025872868	0.022302348	51552/394/5868/26225/5861/5870/55207/22931	8
GO:0019001	MF	Guanyl nucleotide binding	8/87	401/18432	0.00061117	0.025872868	0.022302348	51552/394/5868/26225/5861/5870/55207/22931	8
GO:0032561	MF	Guanyl ribonucleotide binding	8/87	401/18432	0.00061117	0.025872868	0.022302348	51552/394/5868/26225/5861/5870/55207/22931	8
GO:0003925	MF	G protein activity	3/87	41/18432	0.00095111	0.030197744	0.02603038	5868/5861/55207	3
GO:0042169	MF	SH2 domain binding	3/87	41/18432	0.00095111	0.030197744	0.02603038	394/1398/5747	3